Isothermal Section of the Ternary Sn-Cu-Ni System and Interfacial Reactions in the Sn-Cu/Ni Couples at 800 °C

CHAO-HONG WANG and SINN-WEN CHEN

The isothermal section of the Sn-Cu-Ni system at 800 °C has been experimentally determined. There is no ternary compound. A solid solution with a very wide compositional range, the γ phase is formed between the Ni_3Sn(H) phase and Cu_4Sn(H) phase; however, both of these two binary phases are not stable at 800 °C. The binary Ni_3Sn_2 phase also has extensive ternary solubility. The homogeneity ranges of both the γ and Ni_3Sn_2 phases are very large in parallel to the Cu-Ni side, but relatively narrow along the Sn direction. This phenomenon indicates that Cu and Ni are exchangeable in both phases. Three kinds of reaction couples, Sn-55 at. pct Cu/Ni, Sn-65 at. pct Cu/Ni, and Sn-75 at. pct Cu/Ni, were prepared and reacted at 800 °C for 5 to 20 minutes. The reaction paths are liquid/Ni_3Sn_2/γ/Ni_3Sn(L)/Ni for the Sn-55 at. pct Cu/Ni and Sn-65 at. pct Cu/Ni couples, and the reaction path is liquid/γ/Ni_3Sn(L)/Ni for the Sn-75 at. pct Ni couples.

I. INTRODUCTION

THIS study determined the isothermal section of the ternary Sn-Cu-Ni system and interfacial reactions in the Sn-Cu/Ni couples at 800 °C. Previously, only very limited results were available regarding phase equilibria of the Sn-Cu-Ni system,[1–7] and there was no literature on interfacial reactions, except for some studies focusing on Sn-0.7 wt pct Cu and related alloys[7,8,9] at low temperatures. Bastow and Kirkwood[2] determined isothermal sections at the Cu corner at 700 °C, 1025 °C, 1050 °C, and 1090 °C. Miki and Ogino,[4] Wachtel and Bayer,[5] and Gupta[6] reported partial Sn-Cu-Ni isothermal sections in the region between the (Cu,Ni) solid solution, Cu_3Sn and Ni_3Sn_2 phases, and Ni_3Sn_2 phase. In addition, Lin *et al.*[7] first determined the entire Sn-Cu-Ni isothermal section at 240 °C. Although the temperatures of these isothermal sections are different, all the results have indicated that there are no ternary compounds, and most of the binary compounds have significant ternary solubility in the Sn-Cu-Ni system.

II. EXPERIMENTAL PROCEDURES

Alloys were prepared with Sn shots (99.9 wt pct), Cu foils (99.9 wt pct), and Ni foils (99.9 wt pct). Proper amounts of pure elements were weighed. For phase-equilibria study, these elements were arc melted together, encapsulated in a quartz tube in a 10^{-3} torr vacuum, and equilibrated at 800 °C for 30 days. After heat treatment, the sample capsule was quenched in water. Annealed specimens were removed from the tube and were cut into half for metallographical analysis and X-ray diffraction analysis. For interfacial-reaction study, Sn shots and Cu foils were sealed in a quartz tube, and the sample capsule was placed in a furnace at 1200 °C for 3 days. Pieces of Sn-Cu alloys were then cut from the quenched Sn-Cu ingots. The Sn-Cu alloys were sealed together with a Ni foil and placed in a furnace at 800 °C. At 800 °C, the Sn-Cu alloys became molten and enclosed the Ni foil. After 5 to 20 minutes, the reaction couples were removed and quenched in ice water. The couples were mounted and the interfaces were metallographically examined. Compositions of the reaction layers were determined by using electron-probe microanalysis (EPMA), and the layer thickness was measured using an optical microscope equipped with an image analyzer.

III. RESULTS AND DISCUSSION

Fifty alloys were prepared and analyzed, with compositions as shown in Table I and Figure 1. Figure 2 is the micrograph of alloy 34 (Sn-40 at. pct Cu-40 at. pct Ni) annealed at 800 °C for 30 days, yielding a two-phase structure. The compositions of the bright and dark phases, determined by using EPMA, are Sn-29.4 at. pct Cu-46.5 at. pct Ni and Sn-75.6 at. pct Cu-20 at. pct Ni, respectively. Together with the XRD results, the bright phase is determined to be the γ-(Ni_3Sn(H), Cu_4Sn(H)) phase and the dark is α-(Cu,Ni) phase. Except for the Ni_3Sn and γ-(Ni_3Sn(H), Cu_4Sn(H)) phases, the diffraction peaks determined in this study were compared with the JCPDS data files for phase identification. Results of Miki and Ogino[4] and Gupta[6] were used for the determination of the Ni_3Sn(L), Ni_3Sn(H), and γ-(Ni_3Sn(H), Cu_4Sn(H)) phases. As shown in Figure 1, α is a continuous solid solution of Cu and Ni phases, with approximately 7 at. pct Sn solubility. Similar results are found for alloys 31 through 49, and they are all in the α-γ two-phase field. Both the Ni_3Sn and Cu_4Sn phases have phase transitions, and (H) and (L) are used to denote the phases stable at higher and lower temperatures, respectively.

The γ phase is a solid solution between the Ni_3Sn(H) phase and the Cu_4Sn(H) phase. Gupta[6] first proposed the formation of a solid phase between these two phases, which were of the same DO_3 structure. At 800 °C, all the Cu-Sn compounds are molten and the binary Cu_4Sn(H) phase is not stable;[10] thus, the γ phase could not extend all the way to the Sn-Cu binary side. The phase-transition temperature of the binary Ni_3Sn phase occurs at 1000 °C,[11] and the Ni_3Sn(H) is not

CHAO-HONG WANG, Graduate Student, and SINN-WEN CHEN, Professor, are with the Department of Chemical Engineering, National Tsing Hua University, Hsin-Chu, Taiwan 300 R.O.C. Contact e-mail: swchen@che.nthu.edu.tw

Manuscript submitted October 24, 2002.

stable at 800 °C, either. Since the structure of γ phase is different from that of the Ni_3Sn(L) phase at 800 °C, a two-phase region must exist to separate the γ phase and the Ni_3Sn(L) phase. Figure 3 is the backscattered electron image (BEI) micrograph of alloy 21 (Sn-7 at. pct Cu-68 at. pct Ni), clearly showing a two-phase microstructure of γ phase and Ni_3Sn(L) phase. Figures 4 and 5 are the BEI micrographs of alloys 28 (Sn-15 at. pct Cu-60 at. pct Ni) and 30 (Sn-10 at. pct Cu-70 at. pct Ni). They are in the α-Ni_3Sn(L) two-phase region and the α-γ-Ni_3Sn(L) tie triangle, respectively. Since the compositions of γ and Ni_3Sn(L) are close, and, furthermore, the atomic weights of Cu and Ni are very close, differentiation between these two phases as shown in Figure 5 is difficult.

Table I. Phase Identification of Alloys Examined in This Study

Number	Alloy Composition, At. Pct	Phases in Equilibrium	Composition, At. Pct		
			Sn	Cu	Ni
1	70 at. pct Sn-10 at. pct Cu-20 at. pct Ni	Ni_3Sn_2	42.4	12.5	45.1
		L	—	—	—
2	60 at. pct Sn-10 at. pct Cu-30 at. pct Ni	Ni_3Sn_2	42.7	11.2	46.1
		L	—	—	—
3	60 at. pct Sn-20 at. pct Cu-20 at. pct Ni	Ni_3Sn_2	42.2	19.9	37.9
		L	—	—	—
4	50 at. pct Sn-10 at. pct Cu-40 at. pct Ni	Ni_3Sn_2	42.3	11	46.7
		L	—	—	—
5	50 at. pct Sn-20 at. pct Cu-30 at. pct Ni	Ni_3Sn_2	42.2	19.9	37.9
		L	—	—	—
6	50 at. pct Sn-30 at. pct Cu-20 at. pct Ni	Ni_3Sn_2	41.7	24.5	33.8
		L	—	—	—
7	50 at. pct Sn-40 at. pct Cu-10 at. pct Ni	Ni_3Sn_2	41.1	27.9	31
		L	—	—	—
8	40 at. pct Sn-40 at. pct Cu-20 at. pct Ni	Ni_3Sn_2	40.3	28.9	30.8
		L	—	—	—
9	40 at. pct Sn-50 at. pct Cu-10 at. pct Ni	Ni_3Sn_2	40.9	29.2	29.9
		L	—	—	—
10	30 at. pct Sn-60 at. pct Cu-10 at. pct Ni	Ni_3Sn_2	38.6	30.1	31.3
		L	—	—	—
11	35 at. pct Sn-5 at. pct Cu-60 at. Ni	γ	25.9	11.2	62.9
		Ni_3Sn_2	37.5	2.8	59.7
12	35 at. pct Sn-10 at. pct Cu-55 at. Ni	γ	25.7	20.9	53.4
		Ni_3Sn_2	37.7	6	56.3
13	35 at. pct Sn-15 at. pct Cu-50 at. pct Ni	γ	25.8	29.5	44.7
		Ni_3Sn_2	37.7	10.2	52.1
14	35 at. pct Sn-20 at. pct Cu-45 at. pct Ni	γ	26	37.5	36.5
		Ni_3Sn_2	37.7	14.2	48.1
15	32.5 at. pct Sn-32.5 at. pct Cu-35 at. pct Ni	γ	25.4	47.9	26.7
		Ni_3Sn_2	37.9	19.7	42.4
		γ	—	—	—
16	30 at. pct Sn-5 at. pct Cu-65 at. pct Ni	Ni_3Sn (L)	—	—	—
		Ni_3Sn_2	37.4	1.6	61
17	30 at. pct Sn-10 at. pct Cu-60 at. pct Ni	γ	25.6	13.2	61.2
		Ni_3Sn_2	37.4	3.7	58.9
18	30 at. pct Sn-30 at. pct Cu-40 at. pct Ni	γ	25.4	38.2	36.4
		Ni_3Sn_2	37.8	14	48.2
19	30 at. pct Sn-40 at. pct Cu-30 at. pct Ni	γ	25.3	50.2	24.5
		Ni_3Sn_2	37.7	21.2	41.1
20	30 at. pct Sn-50 at. pct Cu-20 at. pct Ni	γ	25.1	60.9	14
		Ni_3Sn_2	37.8	29.2	33
21	25 at. pct Sn-7 at. pct Cu-68 at. pct Ni	γ	—	—	—
		Ni_3Sn(L)	—	—	—
22	25 at. pct Sn-15 at. pct Cu-60 at. pct Ni	γ	—	—	—
23	25 at. pct Sn-20 at. pct Cu-55 at. pct Ni	γ	—	—	—
24	25 at. pct Sn-30 at. pct Cu-45 at. pct Ni	γ	—	—	—
25	25 at. pct Sn-40 at. pct Cu-35 at. pct Ni	γ	—	—	—
26	20 at. pct Sn-75 at. pct Cu-5 at. pct Ni	γ	—	—	—
27	10 at. pct Sn-5 at. pct Cu-85 at. pct Ni	α-(Cu,Ni)	8.2	5.1	86.7
		Ni_3Sn(L)	23.9	2.2	73.9
28	10 at. pct Sn-10 at. pct Cu-80 at. pct Ni	α-(Cu,Ni)	8.6	10.5	80.9
		Ni_3Sn(L)	23.8	4.3	71.9
29	10 at. pct Sn-15 at. pct Cu-75 at. pct Ni	α-(Cu,Ni)	9	15.5	75.5
		Ni_3Sn(L)	23.8	6	70.2

Table I. Continued. Phase Identification of Alloys Examined in This Study

Number	Alloy Composition, At. Pct	Phases in Equilibrium	Composition, At. Pct		
			Sn	Cu	Ni
30	20 at. pct Sn-10 at. pct Cu-70 at. pct Ni	α-(Cu,Ni)	8.5	16.2	75.3
		Ni_3Sn(L)	—	—	—
		γ	—	—	—
31	20 at. pct Sn-15 at. pct Cu-65 at. pct Ni	α-(Cu,Ni)	8.8	22.6	68.6
		γ	24.3	11.9	63.8
32	20 at. pct Sn-20 at. pct Cu-60 at. pct Ni	α-(Cu,Ni)	7.9	33.4	58.7
		γ	24.3	14.5	61.2
33	20 at. pct Sn-30 at. pct Cu-50 at. pct Ni	α-(Cu,Ni)	5.3	58.7	36
		γ	24.3	20.9	54.8
34	20 at. pct Sn-40 at. pct Cu-40 at. pct Ni	α-(Cu,Ni)	4.4	75.6	20
		γ	24.1	29.4	46.5
35	20 at. pct Sn-50 at. pct Cu-30 at. pct Ni	α-(Cu,Ni)	5.2	83.1	11.7
		γ	24.3	39.4	36.3
36	20 at. pct Sn-60 at. pct Cu-20 at. pct Ni	α-(Cu,Ni)	7.3	85.4	7.3
		γ	23.1	53.7	23.2
37	20 at. pct Sn-65 at. pct Cu-15 at. pct Ni	α-(Cu,Ni)	8	86.4	5.6
		γ	22.9	59.9	17.2
38	20 at. pct Sn-70 at. pct Cu-10 at. pct Ni	α-(Cu,Ni)	8	88.1	3.9
		γ	22	67.3	10.7
39	15 at. pct Sn-30 at. pct Cu-55 at. pct Ni	α-(Cu,Ni)	6.9	41.4	51.7
		γ	23.8	17.6	58.6
40	15 at. pct Sn-70 at. pct Cu-15 at. pct Ni	α-(Cu,Ni)	7.4	85	7.6
		γ	23.6	52.6	23.8
41	15 at. pct Sn-75 at. pct Cu-10 at. pct Ni	α-(Cu,Ni)	8.2	86.6	5.2
		γ	22.7	61	16.3
42	15 at. pct Sn-80 at. pct Cu-5 at. pct Ni	α-(Cu,Ni)	—	—	—
		γ	—	—	—
43	15 at. pct Sn-82.5 at. pct Cu-2.5 at. pct Ni	α-(Cu,Ni)	—	—	—
		γ	16.8	81.3	1.9
44	10 at. pct Sn-20 at. pct Cu-70 at. pct Ni	α-(Cu,Ni)	8.7	20.4	70.9
		γ	24.4	11.1	64.5
45	10 at. pct Sn-30 at. pct Cu-60 at. pct Ni	α-(Cu,Ni)	7.8	32.4	59.8
		γ	24.1	15	60.9
46	10 at. pct Sn-40 at. pct Cu-50 at. pct Ni	α-(Cu,Ni)	6.4	45.6	48
		γ	23.5	18.5	58
47	10 at. pct Sn-70 at. pct Cu-20 at. pct Ni	α-(Cu,Ni)	5	81.1	13.9
		γ	24.5	35.7	39.8
48	10 at. pct Sn-82.5 at. pct Cu-7.5 at. pct Ni	α-(Cu,Ni)	7.9	86.1	6
		γ	23.2	58	18.8
49	10 at. pct Sn-85 at. pct Cu-5 at. pct Ni	α-(Cu,Ni)	8.2	87.5	4.3
		γ	22.3	64.6	13.1
50	10 at. pct Sn-87.5 at. pct Cu-2.5 at. pct Ni	α-(Cu,Ni)	8	89.1	2.9
		L	—	—	—
51	28 at. pct Sn-60 at. pct Cu-12 at. pct Ni	Ni_3Sn_2	38.4	30.3	31.3
		γ	26.1	61.1	12.8
		L	—	—	—
52	28 at. pct Sn-62 at. pct Cu-10 at. pct Ni	Ni_3Sn_2	38.6	30.1	31.3
		γ	25.9	61.5	12.6
		L	—	—	—
53	25 at. pct Sn-70 at. pct Cu-5 at. pct Ni	γ	25.3	66	8.7
		L	—	—	—
54	24 at. pct Sn-71 at. pct Cu-5 at. pct Ni	γ	24.8	66.6	8.6
		L	—	—	—

Figure 6 is the BEI micrograph of alloy 19 (Sn-40 at. pct Cu-30 at. pct Ni). The composition of the bright phase is Sn-21.2 at. pct Cu-41.1 at. pct Ni, and that of the continuous dark phase is Sn-50.2 at. pct Cu-24.5 at. pct Ni. These are the Ni_3Sn_2 phase and γ-(Ni_3Sn(H), Cu_4Sn(H)) phase, respectively. Similar results are found for alloys 11 through 20, all of which are in the Ni_3Sn_2-γ two-phase field. The micrograph of alloy 16 (Sn-5 at. pct Cu-65 at. pct Ni), shown in Figure 7, reveals a three-phase microstructure. Here, the large bright phase is the Ni_3Sn_2 phase, just as that shown in Figure 6; however, the continuous phase is now a two-phase mixture of γ phase and Ni_3Sn(L) phase. As mentioned previously, due to the similarities between the γ phase and Ni_3Sn(L) phase, a clear differentiation is difficult.

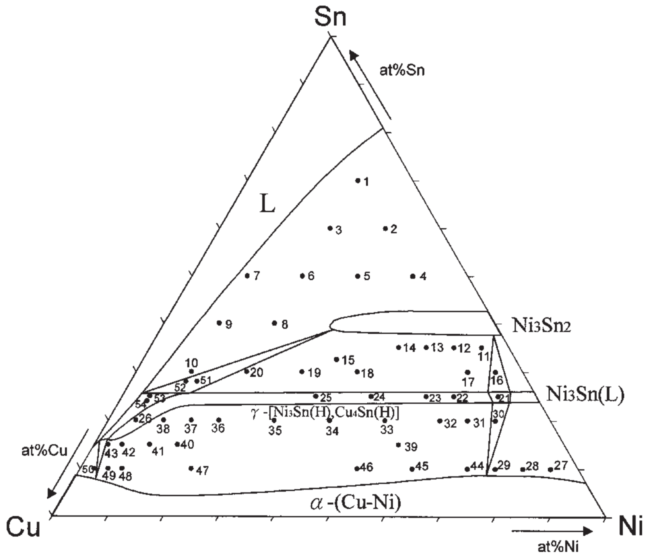

Fig. 1—Sn-Cu-Ni alloys examined in this study superimposed on the proposed isothermal section of Sn-Cu-Ni system at 800 °C.

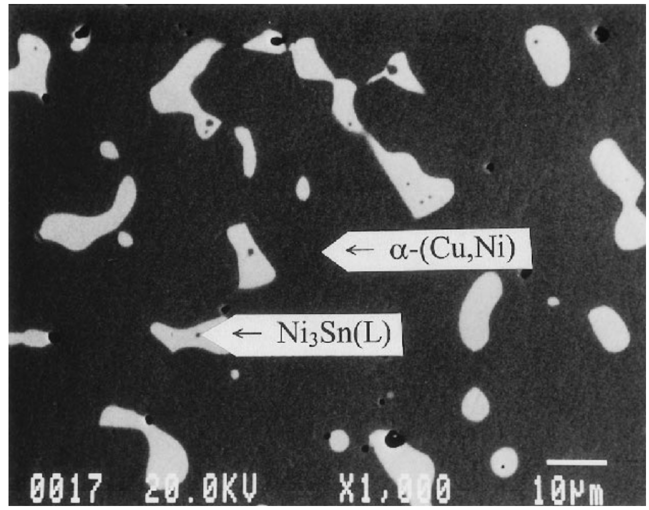

Fig. 4—BEI micrograph of alloy 28 (Sn-10 at. pct Cu-80 at. pct Ni).

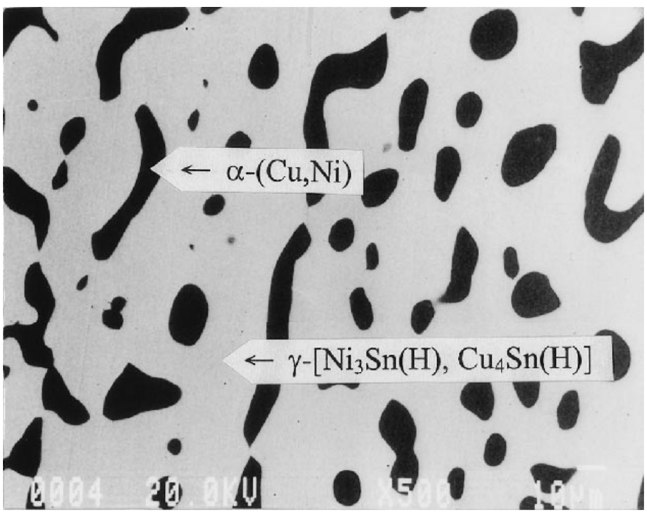

Fig. 2—BEI micrograph of alloy 34 (Sn-40 at. pct Cu-40 at. pct Ni).

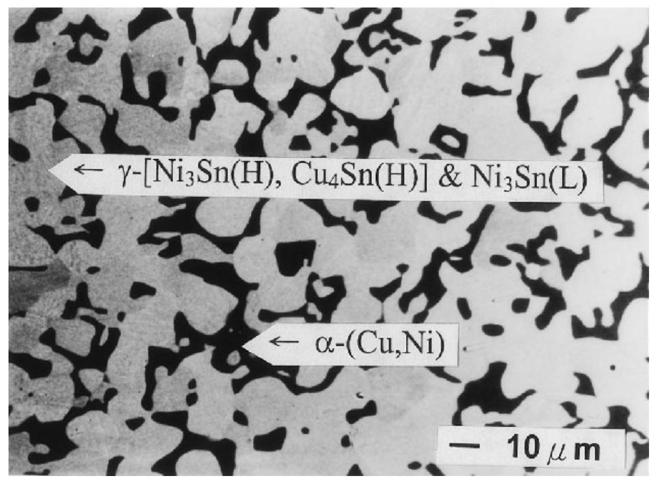

Fig. 5—BEI micrograph of alloy 30 (Sn-10 at. pct Cu-70 at. pct Ni).

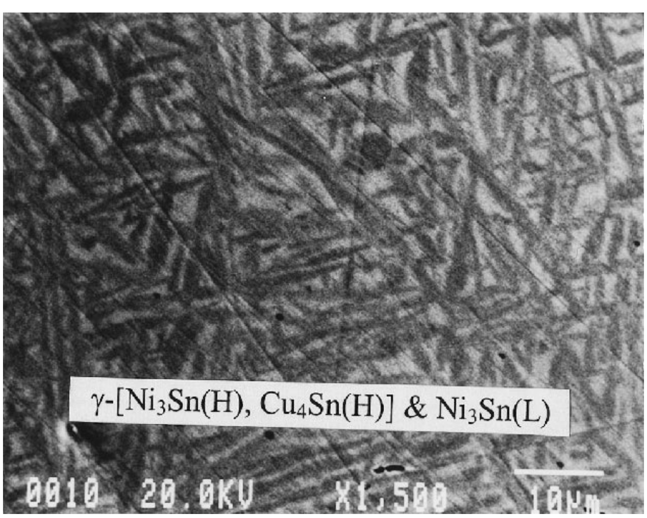

Fig. 3—BEI micrograph of alloy 21 (Sn-7 at. pct Cu-68 at. pct Ni).

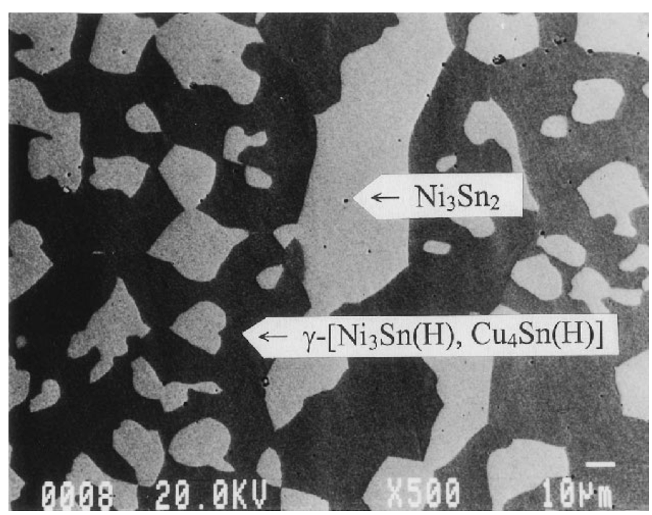

Fig. 6—BEI micrograph of alloy 19 (Sn-40 at. pct Cu-30 at. pct Ni).

Figure 8 is the micrograph of alloy 1 (Sn-10 at. pct Cu-20 at. pct Ni). The large phase is determined to be the Ni_3Sn_2 phase. Although there is more than one phase in the matrix region, morphological observation and related information of phase equilibria all suggest that the matrix is a liquid phase prior to quenching. Similar results have been found for alloys 2 through 10, which are all in the liquid-Ni_3Sn_2 two-phase field at 800 °C. Figure 9 is the optical micrograph of alloy 50 (Sn-87.5 at. pct Cu-2.5 at. pct Ni). Results of compositional analysis identify the large phase as the α phase. An optical micrograph is used instead of scanning electron microscope (SEM) pictures, as for other alloys, because the α phase is too large and a clear SEM picture is very difficult to obtain with such low magnification. In fact, the α phase grows enormously large and can even be distinguished by the naked eye. Figure 10 is the micrograph of alloy 52 (Sn-62 at. pct Cu-10 at. pct Ni). Similar to those shown in Figures 8 and 9, a fine-structure region which is the liquid phase prior to quenching can be observed. However, unlike the two previous pictures, two large phases are observed for alloy 52. The dark phase is the γ phase, and the bright phase is the Ni_3Sn_2 phase. Similar results are found for alloy 51, and both alloys 51 and 52 are in the L + Ni_3Sn_2 + γ tie triangle.

Based on the phase-formation results experimentally determined in this study and the phase diagrams of the three constituent binary systems,[10,11,12] the isothermal section of the Sn-Cu-Ni ternary system at 800 °C is proposed, as shown in Figure 1. The proposed isothermal section is in agreement with most of the literature. No ternary compounds are found in this study; however, most of the binary phases have extensive ternary solubilities. The Cu solubility in the binary Ni_3Sn_2 phase is as high as 33 at. pct. The γ phase is almost a continuous solid solution, except on both binary ends. It can also be noticed that the homogeneity ranges of the α, γ, and Ni_3Sn_2 phases are all very large in parallel to the Cu-Ni side, but are relatively narrow along the Sn direction. This phenomenon indicates that Cu and Ni are exchangeable in all three phases.

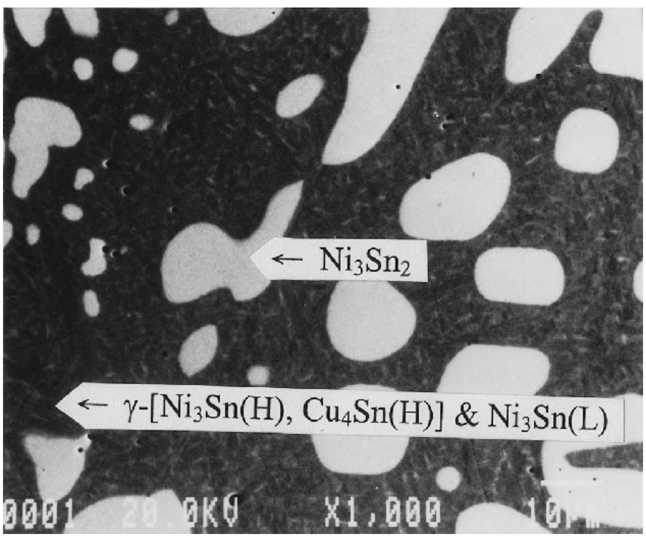

Fig. 7—BEI micrograph of alloy 16 (Sn-5 at. pct Cu-65 at. pct Ni).

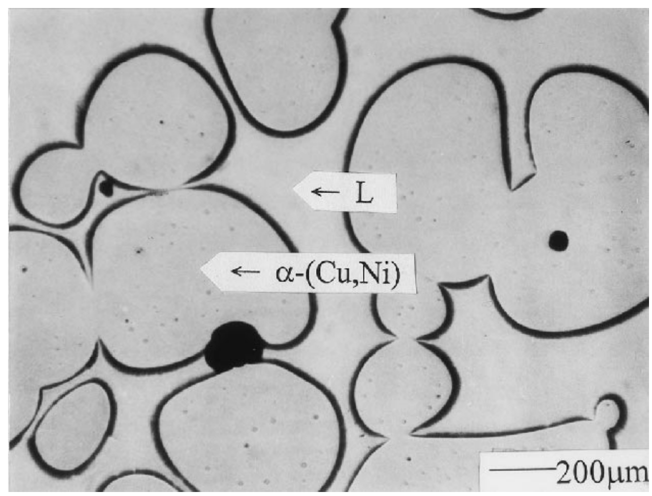

Fig. 9—Optical micrograph of alloy 50 (Sn-87.5 at. pct Cu-2.5 at. pct Ni).

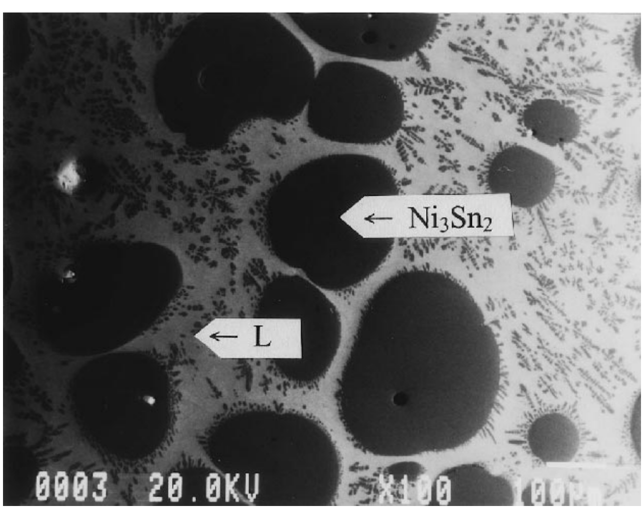

Fig. 8—BEI micrograph of alloy 1 (Sn-10 at. pct Cu-20 at. pct Ni).

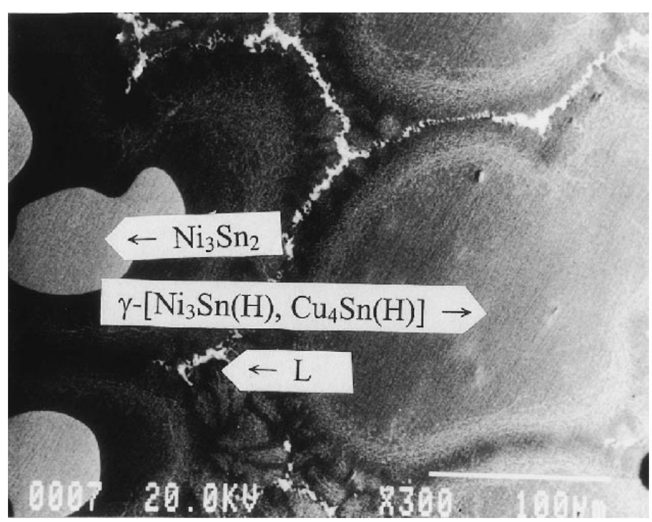

Fig. 10—BEI micrograph of alloy 52 (Sn-62 at. pct Cu-10 at. pct Ni).

In addition to the isothermal-section determination, three different kinds of reaction couples were prepared and examined, *i.e.*, Sn-55 at. pct Cu/Ni, Sn-65 at. pct Cu/Ni, and Sn-75 at. pct Cu/Ni. Figure 11 is the BEI micrograph of the Sn-65 at. pct Cu/Ni couple reacted at 800 °C for 10 minutes. The gray phase adjacent to the dark Ni substrate is the Ni_3Sn compound. The brighter phase with a wavy interface on the left-hand side is the γ and the Ni_3Sn_2(L) phases, although it appeared as one phase. Compositional analysis has indicated that the relative contents between Cu and Ni varied along the reaction layer. The phase-mixture region on the left-hand side has the Ni_3Sn_2, Cu_6Sn_5, Cu_3Sn, and Sn phases. The nickel dissolved into the molten solder, when the nickel and solder were in contact at 800 °C holding, and the molten binary Sn-Cu alloy became a ternary Sn-Cu-Ni melt. The ternary liquid phase solidified and formed various solid phases during cooling. The reaction path of the Sn-65 at. pct Cu/Ni couple is, thus, liquid/Ni_3Sn_2/γ/Ni_3Sn(L)/Ni and is shown in Figure 12. Similar results are found for Sn-65 at. pct Cu/Ni couples reacted for 5, 15, and 20 minutes, except that the layers are thicker with longer reaction times.

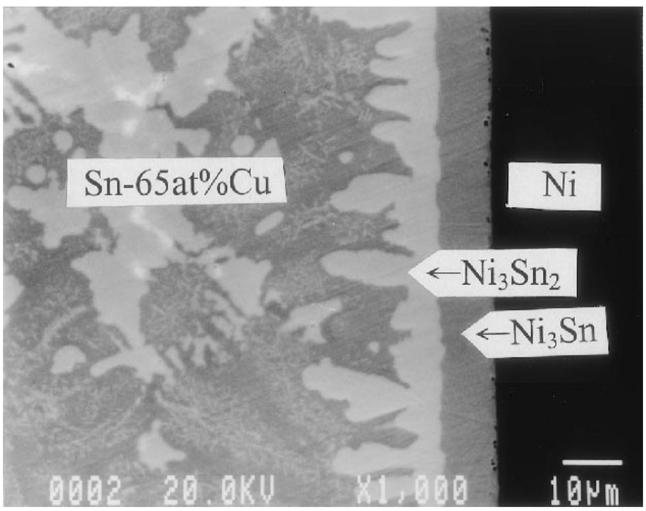

Fig. 11—BEI micrograph of Sn-65 at. pct Cu/Ni at 800 °C for 10 min.

Similar results are found for the Sn-55 at. pct Cu/Ni couples as well. The reaction path is identical to that in the Sn-65 at. pct Cu/Ni couples and is liquid/Ni_3Sn_2/γ/Ni_3Sn(L)/Ni. A noticeable difference between the two kinds of reaction couples is that the growth rates of the reaction layers are higher in the Sn-55 at. pct Cu/Ni couples. However, for the Sn-75 at. pct Cu/Ni couple reacted at 800 °C, as shown in Figure 13, a very different microstructure was formed. From the left-to right-hand sides in the micrograph, the five different regions are Ni, Ni_3Sn, Ni_3Sn_2, Cu_3Sn, and the solidified melt, respectively. A significant feature in Figure 13 is the very thick Cu_3Sn layer and its planar morphology. Its composition is Sn-56.2 at. pct Cu-18.5 at. pct Ni. Since the Cu_3Sn phase is not stable at 800 °C, it is probably formed during cooling when the couple was removed from the furnace. Similar results were found for the Sn-75 at. pct Cu/Ni couple reacted at 800 °C for other lengths of reaction times.

It is still not clear what is the cause for the very dramatic microstructure change, from the wavy and finger-type mixture to the planar-layer structure. One possible explanation is that the reaction paths are different and the path is liquid/γ/Ni_3Sn(L)/Ni in the Sn-75 at. pct Cu/Ni couples. As can be seen on the isothermal section shown in Figure 1, the Cu content of one corner of the L-γ-Ni_3Sn_2 tie triangle is 71 at. pct, and the Sn-75 at. pct Cu is on a different side of the tie-triangle corner from the Sn-55 at. pct Cu and Sn-65 at. pct Cu. Thus, the molten Sn-75 at. pct Cu at 800 °C is likely to be in direct contact with the γ phase, not the Ni_3Sn_2 phase, as for the Sn-55 at. pct Cu and Sn-65 at. pct Cu melt. Nickel dissolved into the Sn-Cu binary melt during isothermal holding. When the couple was removed from the furnace, some of the excess Ni precipitated first as the Ni_3Sn_2 phase on the γ phase first, although most of the nickel in the liquid was retained in the Cu_3Sn

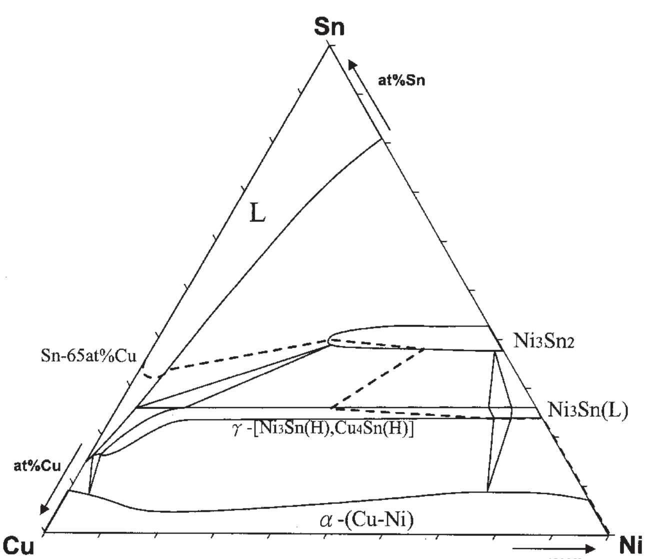

Fig. 12—Reaction path of Sn-65 at. pct Cu/Ni at 800 °C for 10 min.

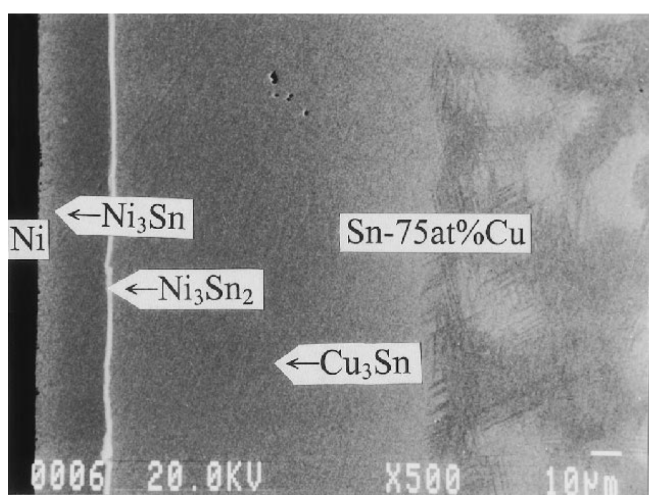

Fig. 13—BEI micrograph of Sn-75 at. pct Cu/Ni at 800 °C for 20 min.

phase. Since the Sn-75 at. pct Cu has exactly the same composition as the Cu_3Sn phase, a thick layer of the Cu_3Sn phase is expected. This presumption that the Ni_3Sn_2 phase is formed during quenching in the Sn-75 at. pct Cu/Ni couple is further supported by the observation that the Ni_3Sn_2 phase is much thinner in the Sn-75 at. pct Cu/Ni couple as compared to that in the other two kinds of couples. However, these are only preliminary analyses, and more interfacial-reaction studies are needed to further verify this explanation.

IV. CONCLUSIONS

The isothermal section of the Sn-Cu-Ni system at 800 °C has been determined. Although there is no ternary compound, most binary compounds of this ternary system at 800 °C all have very extensive ternary solubility. Results of interfacial reactions are similar in the Sn-55 at. pct Cu/Ni and Sn-65 at. pct Cu/Ni couples, and both their reaction paths are liquid/Ni_3Sn_2/γ/Ni_3Sn(L)/Ni. A dissimilar microstructure is found in the Sn-75 at. pct Cu/Ni couples. It is presumed that the reaction path is different and is liquid/γ/Ni_3Sn(L)/Ni.

ACKNOWLEDGMENT

The authors acknowledge the financial support of the National Science Council, Taiwan, through Project No. NSC89-2623-7-007-007.

REFERENCES

1. J.T. Eash and C. Upthegrove: *Trans. AIME*, 1933, vol. 104, pp. 221-49.
2. B.D. Bastow and D.H. Kirkwood: *J. Inst. Met*., 1971, vol. 99, pp. 277-83.
3. Y. Murakami and S. Kachi: *Trans. JIM*, 1983, vol. 24 (1), pp. 9-17.
4. M. Miki and Y. Ogino: *Trans. JIM*, 1984, vol. 2 (9), pp. 593-602.
5. E. Wachtel and E. Bayer: *Z. Metallkd*., 1984, vol. 75, pp. 61-69.
6. K.P. Gupta: *Ind. Inst. Met*., 1990, vol. 1, pp. 195-218.
7. C.-H. Lin, S.-W. Chen, and C.-H. Wang: *J. Electronic Mater*., 2002, vol. 31 (9), pp. 907-15.
8. D.R. Frear, J.W. Jang, J.K. Lin, and C. Zhang: *JOM*, 2001, vol. 53 (6), p. 28.
9. W.T. Chen, C.E. Ho, and C.R. Kao: *J. Mater. Res*., 2002, vol. 17 (2), pp. 263-66.
10. N. Saunders and A.P. Miodownik: *Binary Alloy Phase Diagrams*, 2nd ed., T.B. Massalski, ed., ASM, Materials Park, 1990, pp. 1481-83.
11. P. Nash and A. Nash: *Binary Alloy Phase Diagrams*, 2nd ed., T.B. Massalski, ed., ASM, Materials Park, 1990, pp. 2863-64.
12. D.J. Charkrabarti, D.E. Laughlin, S.-W. Chen, and Y.A. Chang: *Binary Alloy Phase Diagrams*, 2nd ed., T.B. Massalski, ed., ASM, Materials Park, 1990, pp. 1442-45.